Journal of Engineering and Sustainable Development
http://jeasd.uomustansiriyah.edu.iq
https://doi.org/10.31272/jeasd.24.6.1

JEASD

Vol. 24 No. 06, November 2020
ISSN 2520-0917

SEISMIC EVALUATION AND RETROFIT ON AN EXISTING HOSPITAL BUILDING

***Husain K. Jarallah[1]** **D. K. Paul[2]** **Yogendra Singh [3]**

1)Department of Civil Engineering, College of Engineering, Mustansiriyah University, Baghdad, Iraq
2)Department of Earthquake Engineering ,Indian Institute of Technology Roorkee، Roorkee 247 667, Roorkee , India
3)Department of Earthquake Engineering ,Indian Institute of Technology Roorkee، Roorkee 247 667,Roorkee , India

Received 18/12/2019 ***Accepted in revised form 21/6/2020*** ***Published 1/11/2020***

Abstract: The nonlinear pushover analysis was used to evaluate an existing 8-storey reinforced concrete framed hospital building under seismic force and presented in this manuscript. The 'Guru Teg Bahadur Hospital' is one of the important hospitals at Delhi-India, it was selected for this research. The three-dimensional frame model was used to model the building with a fixed base. The beams and columns were modeled by using three-dimension line frame elements with the centre lines joined at nodes. Diagonal strut elements were used to model the brick masonry infills. The slabs were considered as rigid diaphragms. The plastic hinge rotation capacities as per Federal Emergency Management Agency 356 (FEMA 356) with Performance Levels were adopted in this study, considering the axial force-moment and shear force-moment interactions. The nonlinear pushover analysis of the selected building was done with infills and it was observed that the infills (due to their small number in the considered building) do not make any appreciable effect on the performance level, except their failure at an early stage. The Capacity Spectrum Method (CSM) and Displacement Coefficient Method (DCM) were used to estimate the performance point of the building. The values of various coefficients as per Federal Emergency Management Agency 440 (FEMA 440) were adopted. The DCM was observed to give slightly higher target displacements, as compared to CSM. It was observed in the nonlinear pushover analysis that the unreinforced masonry (URM) infills collapse before the performance point of the building for the Maximum Considered Earthquake (MCE). As the intervention inside the functioning hospital is extremely difficult, it was explored whether it is possible to safeguard the infills by stiffening the building by providing external buttresses. Two cases of retrofitting schemes with 1.2m wide and 3m wide buttresses in transverse direction were used and analysed. It was found that this is not a practicable approach, as the infills collapse even with 3m wide buttresses.

Keywords: *capacity spectrum method, displacement coefficient method, nonlinear pushover analysis, target displacement, masonry infills, drift, buttresses.*

1. Introduction

Serious casualties and losses may be resulted from the collapse of existing hospital buildings under a severe earthquake, whereas, hospital buildings are expected to be functional after an earthquake. Many existing buildings in India are severely deficient against earthquake effect and the number of such buildings is growing rapidly. This was marked in the past earthquakes [1]. To avoid the damage and casualties due to the failure of hospital buildings under earthquake, all hospital buildings should be evaluated, so that hospital buildings with a lack of seismic performance can be retrofitted. Seismic capacity evaluation and retrofit of existing buildings are a much more challenging task than the design of

**Corresponding Author*: khalfdce@uomustansiriyah.edu.iq

a new building and are play an important role to avoid the collapse of the building during an earthquake. The Guru Teg Bahadur Hospital (commonly known as G.T.B. Hospital) is a big hospital in the National Capital Region (NCR) of India catering to a large population in the eastern zone of Delhi and its neighboring state, viz. Uttar Pradesh (being located at the Delhi-Uttar Pradesh border). The ward block building of this hospital was built in 1982 for 500 patient beds. The building was built in two stages. The first stage was built in 80's (6 storeys) and the second stage was built in the mid 90's (top 2 storeys). Presently, it has adjusted more than 1000 beds due to an acute shortage of beds. The ward building is 8 storey building with having plinth area of about 18000 m^2. The building is divided into 6 parts separated by expansion joints as the structural arrangement for the building as shown in Fig. (1). The north and south portions of the building are the wards. The opposite wards are connected through two corridor blocks on the Eastern and Western ends of the wards. There is an open courtyard at the center of this rectangular building. Each block separated by expansion joints is more or less symmetric. The whole building's outer dimensions are about, 65m x 58m. Each ward has overall plan dimensions of 14m x 58m and is rectangular in plan, which is further divided into 2 parts, each of these parts is approximate 14m x 29m. The connecting corridor is 65 m in length but the width varies as stair case and lift lobby consisting of two lifts are also located in each corridor. The typical storey height is 3.35 m (the plinth level height is 2.5 m). A single ward consisting of two blocks, separated by an expansion joint, was considered in this study. The nonlinear pushover analysis of the building is predicted by using a proprietary computer programme ETABS [2]. The performance-based analysis as per FEMA 356/273[3, 4] and ATC40 [5] was also performed. The target displacement method and the capacity spectrum method was used to capture the performance level of the building.

2. The Structure

The ward blocks are founded on a raft foundation resting on the sandy soil of medium stiffness. The foundation with 1.05 m thickness was designed for bearing capacity of 196 kN/m^2 at a depth of 2.5 m below the original ground level. The reinforced concrete slab and concrete beams are supported by concrete columns, those are the structure system that it is carried all structural weight and superimposed load on the building. The concrete slab is 130 mm thick at all floors. The typical framing consists of columns spaced at 3.20 m c/c in the longitudinal direction and 4.13, 2.82 and 7.07 m c/c in the transverse direction. The clear gap between the two adjacent blocks is 0.42 m. Figure (2) shows the plan of a typical wing (only the primary elements are shown here) of the ward blocks with the orientation of the columns and the floor framing plan. The beam-column frames are represented as the seismic force-resisting system. The beams (400mm x 500mm) and columns (400mm x 600mm) sizes are the same at all the floors. The columns have the same reinforcement details for every two successive storeys. There is sufficient development length for columns located at ground floor reinforcement into the raft, this is obtained from the reinforcement details given in the drawings provided by Superintendent Engineers of G.T.B. Hospital, these columns are cast at site monolithic with the raft.

3. Material

Table 1 presents the properties of concrete and steel reinforcement obtained from available drawings [6]. The specified material strength can be lower than the actual (expected) strength

of the in-situ material, therefore, the "expected" values are always larger than the "specified" values because of the inherent overstrength in the original material and strength gained over time (FEMA 273[4]).

Table 1. Properties of Construction Materials

Concrete		
Member	Column	Beam
Grade	M25	M15
Specified cylinder strength (MPa)	20	12
Expected cylinder strength (MPa)	25.6	16.8
Steel Reinforcement		
Yield strength(MPa)	415	
Expected yield strength(MPa)	497	
Masonry Infill		
Expected compressive strength(MPa)	5.4	

4. Modelling and Analysis

The nonlinear static pushover analysis was used to capture the performance level of the building, therefore, the development of the force-deformation curve for the critical sections of beams, columns, infills walls and shear wall was developed. The computer model of the building was developed in ETABS [2]. Gravity load and the corresponding masses coming from these members were considered.

4.1. Modeling

Three dimension line frame elements were used to model the beams and columns with the centerlines joined at nodes. Figure 3 shows the three-dimensional computer model of the building. Cracked section stiffness as per FEMA 356 [3] was used for modelling the initial stiffness of the structure. Table 2 presents member stiffness used in the analysis.

Table 2. Component initial stiffness

Component	Flexural rigidity	Shear rigidity	Axial rigidity
Beam	0.5 Ec Ig	0.4 Ec Aw	Ec Ag
Column	0.7 Ec Ig	0.4 Ec Aw	Ec Ag

The rigid beam-column joints were modelled by giving end offsets at the joints. A rigid zone factor of 1.0 was taken. The influence of horizontal diaphragms action of the floor slabs was used in the floor slabs in the global action and deformation capacity of the building. The tributary area as per IS 456:2000 [7] having triangular and trapezoidal segments was used to distribute the weight of the slab to the supporting beams. In the model, fixity was considered at the top of the raft. The effect of soil-structure interaction was not considered in the analyses. The two adjacent blocks are separated by expansion joints of 20 mm. The expansion joint provided is not sufficient to serve the purpose of the seismic joint (i.e. to accommodate the displacement of the building blocks on the two sides) and therefore, it was suggested to join the two parts of the building at each floor level to avoid damage due to pounding of the two blocks. The brick masonry infills, with the location given in Fig. 4, were modeled as strut elements. The weight of the brick masonry infill was assumed to act as uniformly distributed loads on the beams. The dead load was multiplied by a factor of 1.1 to consider the uncertainties in the estimation of the load (ASCE 41[8]). The effect of the live load was not considered in combination with earthquake load. It is assumed that the live load present at the time of earthquake will be taken care of by the 10% increase in the dead load. The pushover analysis is done for the gravity loads incrementally under load control. The displacement control was used to obtain the lateral nonlinear pushover analysis in X (PUSH-X) and Y (PUSH-Y) directions of the building and it was followed the gravity pushover. The collapse mechanism was developed by pushing the building to failure due to the earthquake force. The capacity curve (Base shear versus Roof displacement) is obtained in X and Y directions.

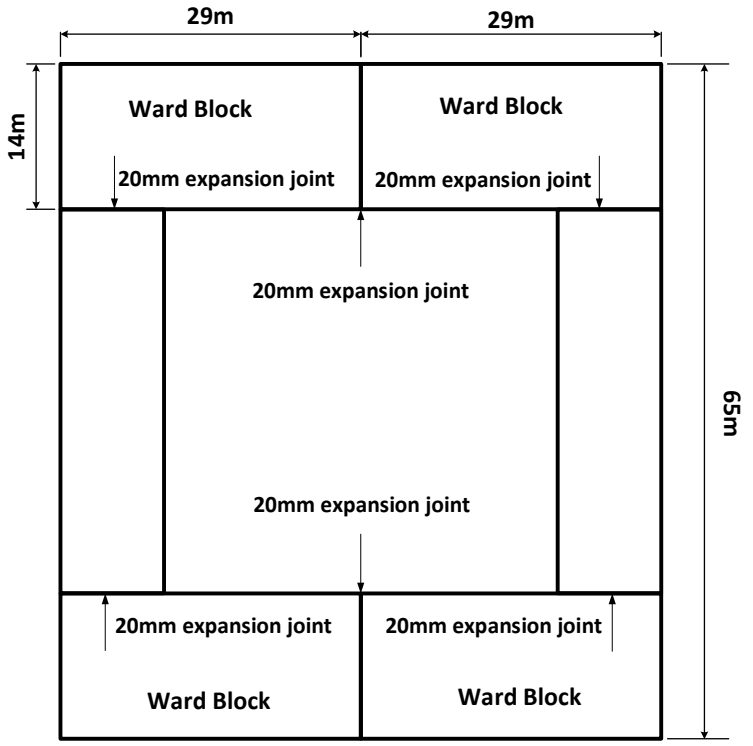

Figure 1. Blocks layout

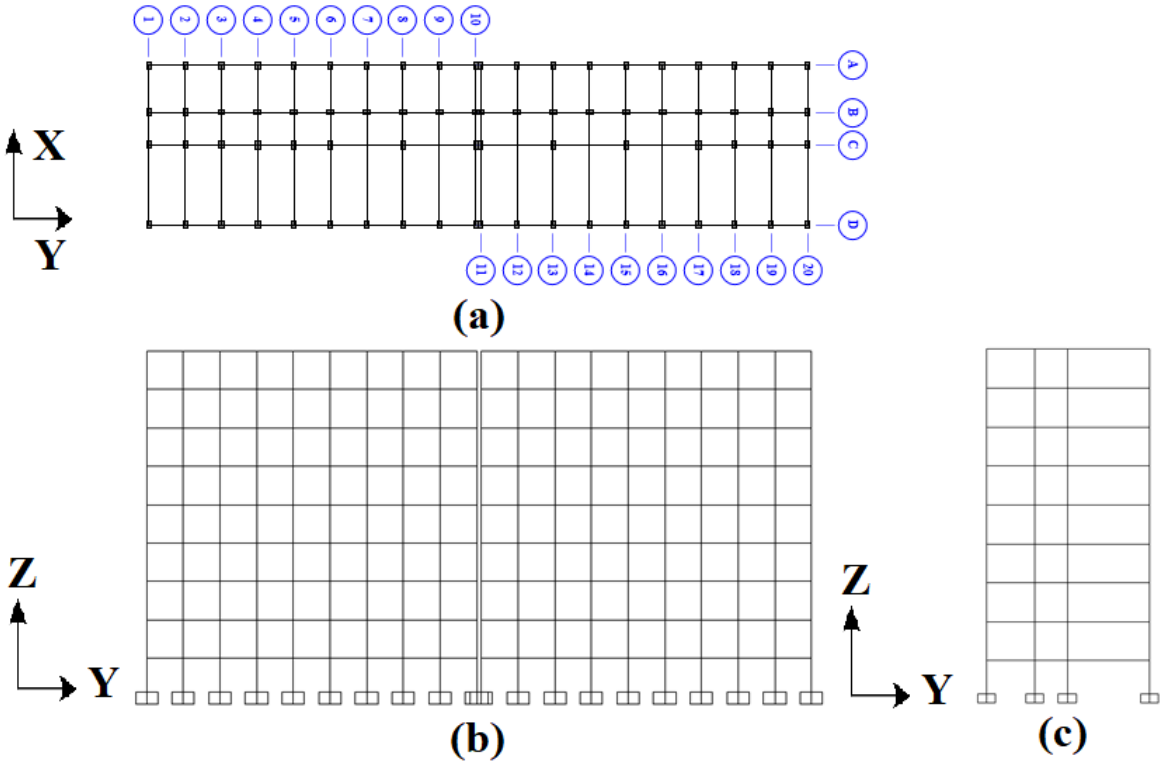

Figure 2. Typical framing system in the building:
(a) Typical Floor Plan; and (b) Typical Longitudinal Elevation Frame
(c) Typical Transverse Elevation Frame

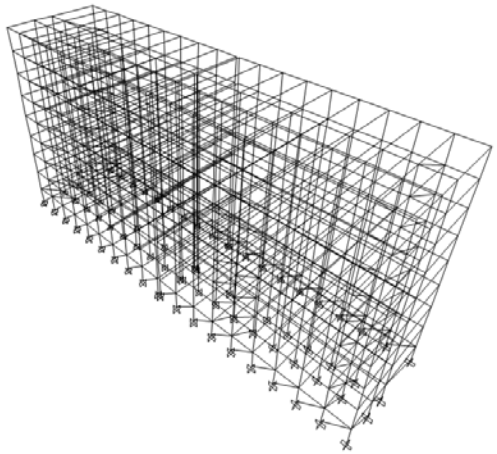

Figure 3. 3D Computer model of the building

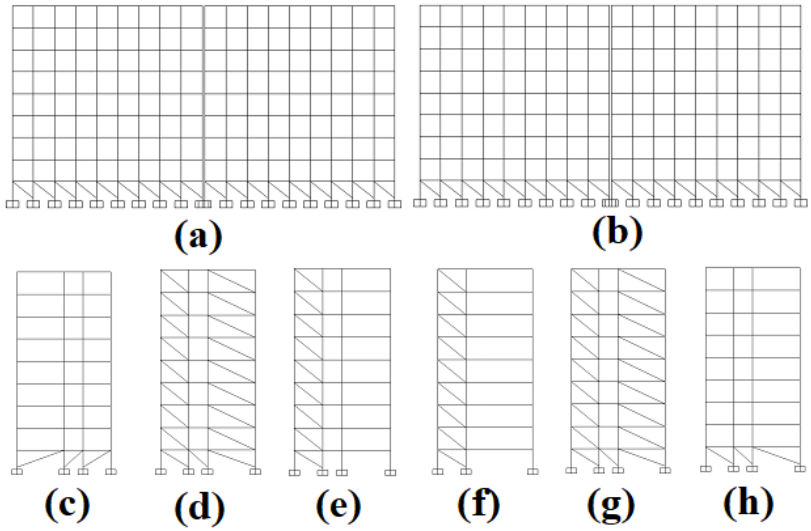

Figure 4 Brick masonry infills location and modelling, (a) along grid A, (b) along grid D, (c) along grid 1, (d) along grid 2, (e) along grid 6, (f) along grid 7, (g) along grid 19,(h) along grid 20

4.2. Nonlinear Static (Pushover) Analysis

The Capacity Spectrum Method (CSM) and Displacement Coefficient Method (DCM) as per FEMA 356 and FEMA 440 [3, 9] were used to capture the seismic performance level of the building. There are two aspects in this method to determine the performance level of a building, the demand placed on the structure during a seismic event, and the capacity of the structure. The performance of the building was measured by its ability to withstand the demand imposed on it during a seismic event. This is accomplished by comparing the anticipated performance of the building to a predetermined performance objective. The determination of the strength/capacity of a building requires a pushover analysis to be performed on the lateral force-resisting system of the building. The pushover analysis determines the level of building lateral forces and corresponding roof displacements that are associated with

successive stages of the development of yielding in the building members.

The target displacement (δ_t) is calculated by the following equation (FEMA 356[3])

$$\delta_t = C_0\, C_1\, C_2\, C_3\, S_a\, \frac{T_e^2}{4\pi^2}\, g \quad (1)$$

where C_o, C_1, C_2 and C_3 are correction factors based on statistical analysis, and are calculated as per FEMA-440 [9]. The effective fundamental period (T_e) of the building is taken in the direction under consideration, accordingly, the spectral acceleration (S_a) is determined with corresponding effective fundamental period and damping ratio in the direction under consideration and g is acceleration value due to gravity.

The nonlinear pushover analysis needs lateral force distribution profile along with the height of the selected building, therefore the lateral force distribution is considered according to the following expression:

$$F_i = \frac{m_i\, h_i^2}{\sum_{j=1}^{n} m_j\, h_j^2} \quad (2)$$

where m_i, m_j are masses of ith or jth floor and h_i, h_j are height of ith or jth floor according to IS 1893:2002 [10] and is shown in Fig. 5. The same distribution of lateral load was considered to perform pushover analyses, independently in two orthogonal directions (X and Y as shown in Fig. 6).

Figure 7 illustrates the axial force-moment interaction diagram for typical perimeter frame columns (A1 and D1) between 3rd and 4th floors. Similar analyses were performed for all the columns. As noted earlier, “expected” values were used for the steel and concrete strength to calculate all capacities. The columns between 3rd and 4th floors (including A1 and D1) typically consist of 16 numbers of 16 mm diameter reinforcement bars. Figure 8 illustrates the moment-curvature diagram of typical 3rd and 4th floor beams (B6-B7) in the longitudinal direction. This beam has 2-ϕ20 and 3-ϕ25 at the top and 5-ϕ20 at the bottom and the confining reinforcement consists of ϕ8 stirrups at 75 mm and 125 mm c/c near the two ends, and at 250 mm c/c in the middle portion of the beam.

4.3. Nonlinear Modelling

The shear and flexural force-deformation back-bone were derived from the details of reinforcement given in the structural drawing and were assigned in all frames elements (columns and primary beams). The beams were assigned with two types of hinges at two ends namely flexural hinges (M3) and shear hinges (V2). While the columns were assigned also with two types of hinges at upper and lower ends namely flexural hinges (PMM) and shear hinges (V2 and V3). A typical force-deformation curve is given in Figure 9. In this figure, Q_{CE} refers to the strength of the component and Q refers to the demand imposed by the earthquake. The points A, B, C, D, and E are marked on the curve: B is the point at which the section yields; at point C, unloading occurs up to point D, which is the point at which the section reaches its residual capacity and then it starts deforming up to point E with a residual capacity. The other salient points are immediate occupancy (IO), life safety (LS) and collapse prevention (CP) that are equally spaced in the region BC. The coordinate values of the B, C, D, E, IO, LS and CP are shown in Fig. 10.

The shear hinges were assigned to all the beam and columns. The shear hinges (V2) were assigned for the beams at two ends. Shear hinges (V2 and V3) were given for all the columns at mid-height taking into account the orientation for the columns. The development of the shear force-deformation curve for the critical sections of beams, columns were obtained by

using the guidelines of FEMA 356 (Tables 6-7 and 6-8). The coordinate values equal to (0, 1.0), (0.003, 1.0), (0.003, 0.2), (0.02, 0.2) were used for B, C, D and E, respectively for beams. Further, the values of plastic rotation corresponding to IO, LS, and CP were used as 0.0015, 0.002, and 0.003, respectively. FEMA 356 does not define the values of plastic deformation for shear in primary columns. Therefore the shear action in columns was modelled as force controlled, by giving very low values (1/100 of those for beams) for plastic deformation corresponding to IO, LS, CP, etc. However, as no shear hinge formation was observed in beams as well as columns, these values have not come into the picture.

4.4. Modelling of Masonry Infills

Masonry infills were modelled as equivalent diagonal compression struts as shown in Fig. 11. The equivalent width of the diagonal member is given as;

$$a = 0.175\left(\lambda_1 h_{col}\right)^{-0.4} r_{\inf} \quad (3)$$

$$\lambda_1 = \left[\frac{E_{me}\, t_{\inf} \sin 2\theta}{4 E_{fe}\, I_{col}\, h_{\inf}}\right]^{0.25} \quad (4)$$

where h_{col} = Column height between centerlines of beams, $h_{\inf}$ = Height of infill panel, E_{fe} = Expected modulus of elasticity of frame material, E_{me} = Expected modulus of elasticity of infill material, I_{col} = Moment of inertia of column, $L_{\inf}$ = Length of infill panel, $r_{\inf}$ = Diagonal length of infill panel, $t_{\inf}$ = Thickness of infill panel and equivalent strut, θ = Angle whose tangent is the infill height to length aspect ratio, in radians , λ_1 = Coefficient used to determine equivalent width of infill strut.

For global building analysis purposes, the stiffness of solid infill panels is represented by using compression struts. The compression struts may be placed concentrically across the diagonals of the frame, effectively forming a concentrically braced frame system (Fig. 11). The effect of the finite width of the strut was considered by checking the column and beam shear capacities against the horizontal and vertical components of the strut forces at yield. FEMA 356 [3] provisions were used for this purpose.

The lower-bound values for masonry compressive strength, elastic modulus in compression, flexural tensile strength, and masonry shear strength based on FEMA 356 [3] were considered and were given in Table 3. Expected strength values for masonry compressive strength, elastic modulus in compression, flexural tensile strength, and masonry shear strength were determined by multiplying lower-bound values by an appropriate factor taken from FEMA 356. This factor is equal to 1.3.

Infill panels were assumed to deflect to nonlinear lateral drifts as given in Table 7-9, FEMA 356 [3]. The parameter d, (Fig. 12) representing nonlinear deformation capacities, is expressed in terms of storey drift ratio as defined in FEMA 356 [3]. For determination of d and the acceptable drift levels using FEMA 356 [3], the ratio of frame to infill strength was determined considering the expected lateral strength of each component.

4.4.1. Plastic Hinge Properties for Infill Strut

The material nonlinearity of the brick masonry infill was considered by assigning the axial hinges (P) in the middle of the strut. The expected modulus of elasticity is 28283MPa of frame material. The dimensions of the equivalent strut and the values of the maximum plastic displacement and yield force for the

brick masonry between A-B, B-C, and C-D respectively are given in Table 3. The axial force-axial deformation curve for brick masonry infill is given in Fig. 13; the values of LS and CP have been calculated from FEMA 356 for fair quality of masonry.

4.4.2. Diagonal Compression Failure of Masonry Infill

The diagonal load at failure is given, as follows, for infill wall;

$$R_{dc} = \frac{0.5\,h\;t\;f_a}{\cos\theta} \qquad (5)$$

where, f_a is the allowable compressive strength, which is reduced from f_c considering the slenderness, t is the thickness of brick masonry infill, h is the height of brick masonry infill . ACI 530 [11] gives the value of f_a the masonry wall as follows.

For $r_{\inf} / t \le 29$

$$f_a = f_c\left(1-\left(\frac{r_{\inf}}{40t}\right)^2\right) \qquad (6)$$

For $r_{\inf} / t > 29$

$$f_a = f_c\left(\frac{20t}{r_{\inf}}\right)^2 \qquad (7)$$

where r_{inf} is the diagonal length of brick masonry infill. The values of R_{dc} different brick masonry infills are given in Fig. 13.

5. Retrofitting Measures Suggested

The safety of the existing structures was checked under the combined effect of gravity and earthquake loads and the results are presented below. It was found that the building framing has Immediate Occupancy (IO) performance level against the MCE earthquake loading, however, the infills fail in in-plane action. As the intervention inside the functioning hospital is extremely difficult, it has explored whether it is possible to safeguard the infills by stiffening the building by providing external buttresses. Two cases of retrofitting schemes with 1.2m wide and 3m wide buttresses in transverse direction were used and analysed.

6. Performance of Building Without and With External Buttresses

The target displacement was calculated by using the Capacity Spectrum Method (CSM) and Displacement Coefficient Method (DCM). The gravity loads were assigned to all the beams and the analysis was performed for the gravity loads (1.1 DL) under load control. When the gravity load analysis is completed, the lateral nonlinear pushover analysis (PUSH-X and PUSH-Y) is started under displacement control. The collapse mechanism of the building was captured by pushing the building in the lateral directions. The capacity curve is representing by the relationship between base shear and roof lateral displacement in the direction under consideration and it is shown in Fig. 14 for X and Y directions. The pushover curve shows that the building has a base shear capacity 15% higher than the design base shear (V_{bx}) calculated for the empirical time period and reduction factor(R) equal to 3, as IS 1893 for the building along the X-direction. In this case, also, the pushover curve shows that the building has base shear capacity almost equal to design base shear (V_{by}) calculated for the empirical time period and reduction factor (R) equal to 3, as IS 1893 for the building along the Y direction (Fig. 15).

The capacity is expressed in an Acceleration Displacement Response Spectrum (ADRS) format in the same plot to check the performance of the building. The capacity

spectra are plotted in the ADRS format in Fig. 16. The figure also shows the performance points for Design Basis Earthquake (DBE) and Maximum Considered Earthquake (MCE) in both directions, using the capacity spectrum method of FEMA 356.

The bilinear representation of the Capacity curves is shown in Fig. 17 for X and Y directions respectively. By using equation (1) the target displacement is given in Table 4 at the MCE earthquake level. Fig. 18 shows the location of the buttresses. The building is strengthened by providing additional buttresses along the transverse direction. The displacements at the roof and base shear at performance level are shown in Table 4 for MCE. The performance points transformed to the plots of base shear versus roof displacement are shown in Fig. 19 for MCE in the X directions with and without buttresses. The hinge status in masonry is shown in Figs. 20-22 for the different cases. The variation of drift ratios along with the height of the building, in the three cases, are given in Fig 23. The drift limit for IO as 0.01 has been used as per ATC-40. The inter storey drift has been checked at each storey and the drift ratio has been found to be less than 0.01

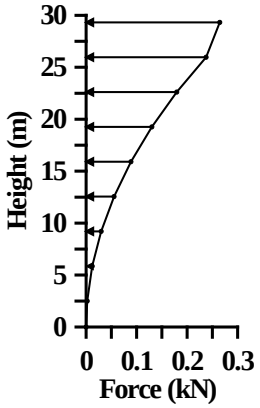

Figure 5. Lateral Load distribution along with height in X and Y direction modelling

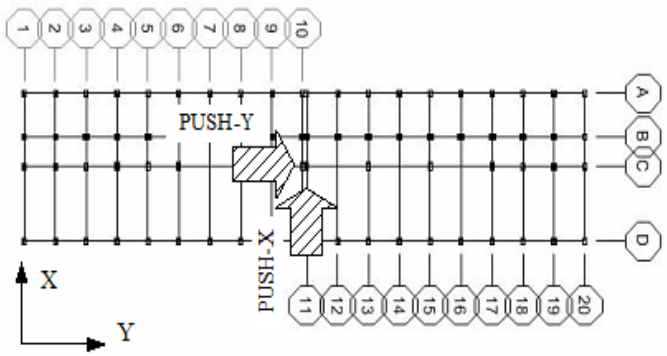

Figure 6 Application of load in pushover analysis

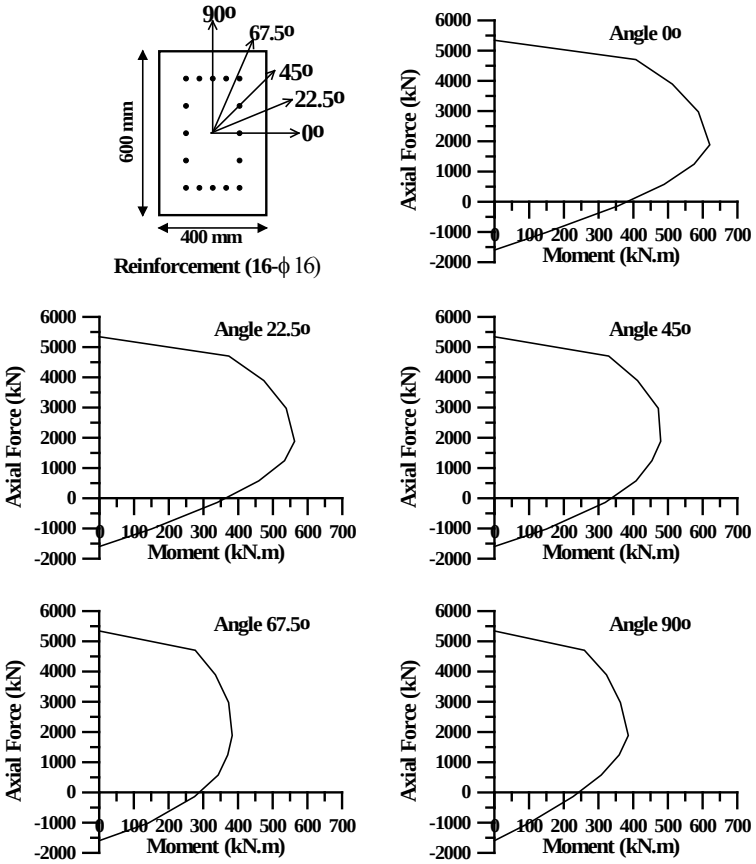

Figure 7 Existing column interaction diagram at 3rd and 4th floors

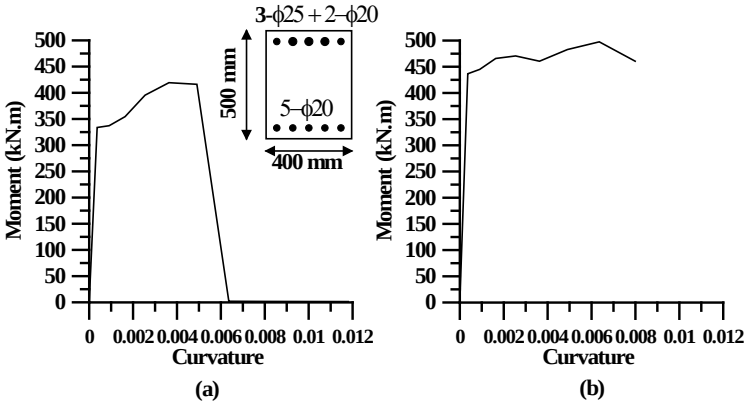

Figure 8. Existing beam moment-curvature diagram at 3rd and 4th floors, (a) Positive Moment (Yield Moment = 333.7 kN.m), (b) Negative Moment (Yield Moment = 436.50 kN.m)

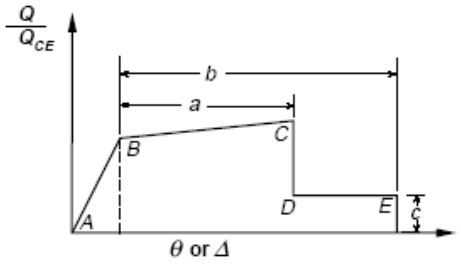

Figure 9. Idealized component load versus deformation curves for depicting component modeling and acceptability (FEMA 356)

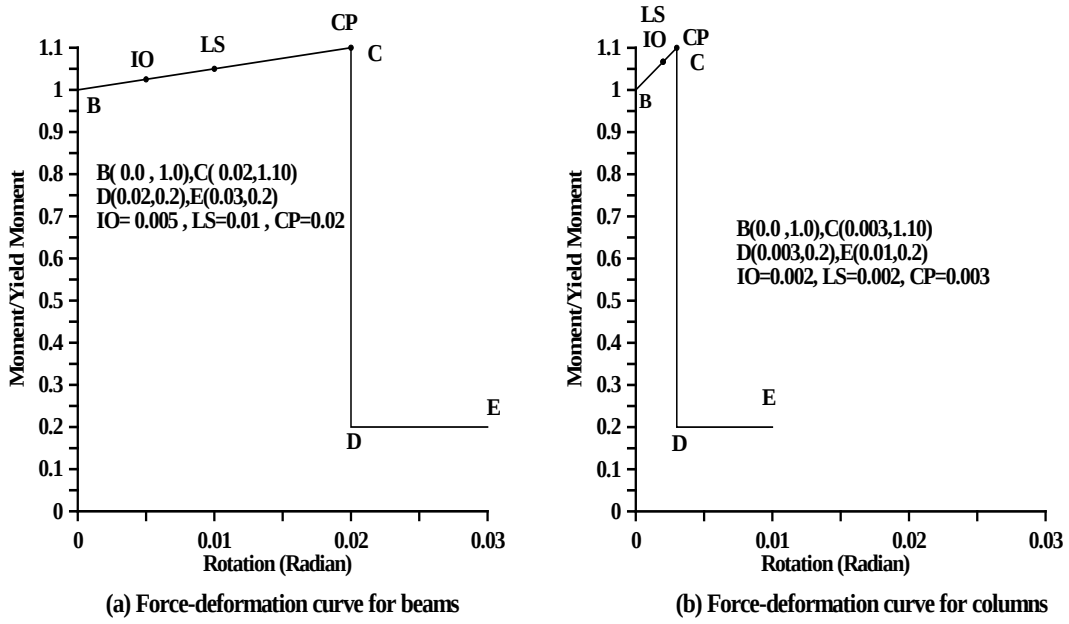

Figure 10. Force-deformation curve for beams and columns

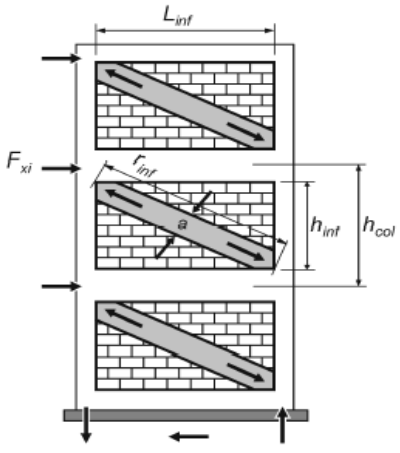

Figure 11. Compression strut analogy–concentric struts (FEMA 356)

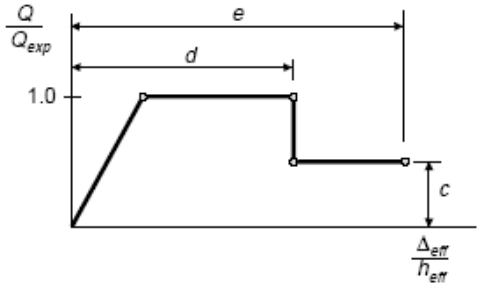

Figure 12. Idealized force-deflection relation for infill panels (FEMA 356)

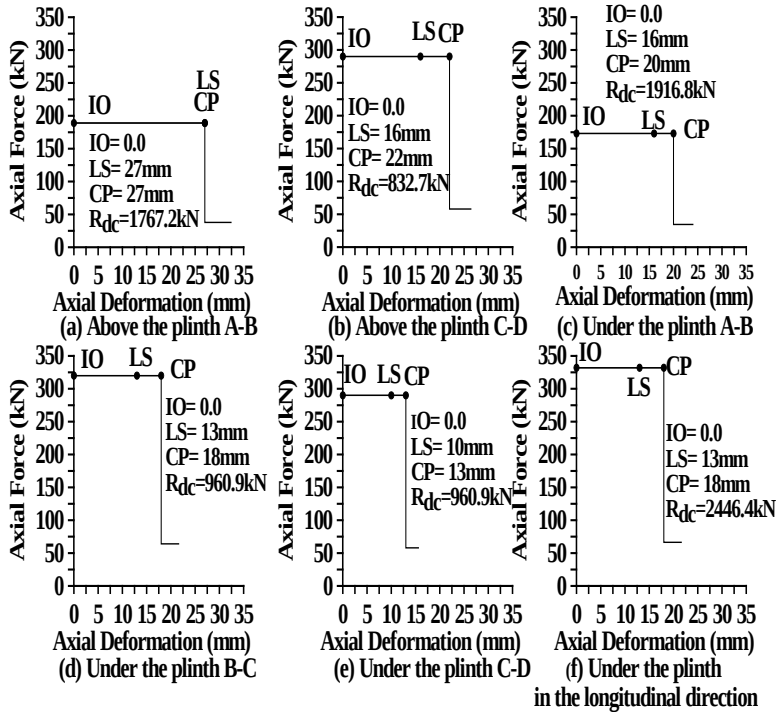

Figure 13. The force-deformation curve for brick masonry

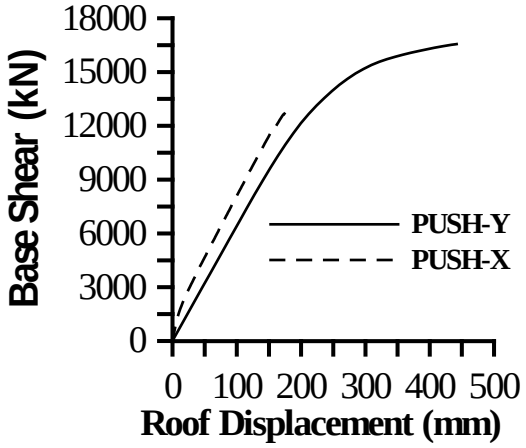

Figure 14. Base shear and roof displacement

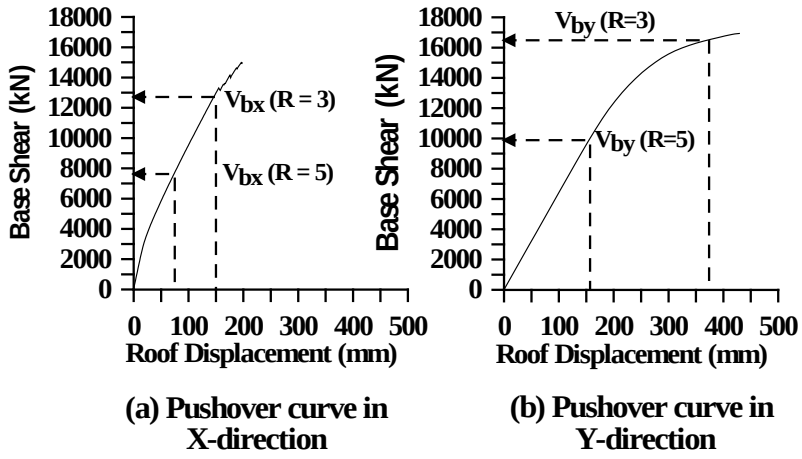

Figure 15. Pushover curve along with X and Y directions with design base share

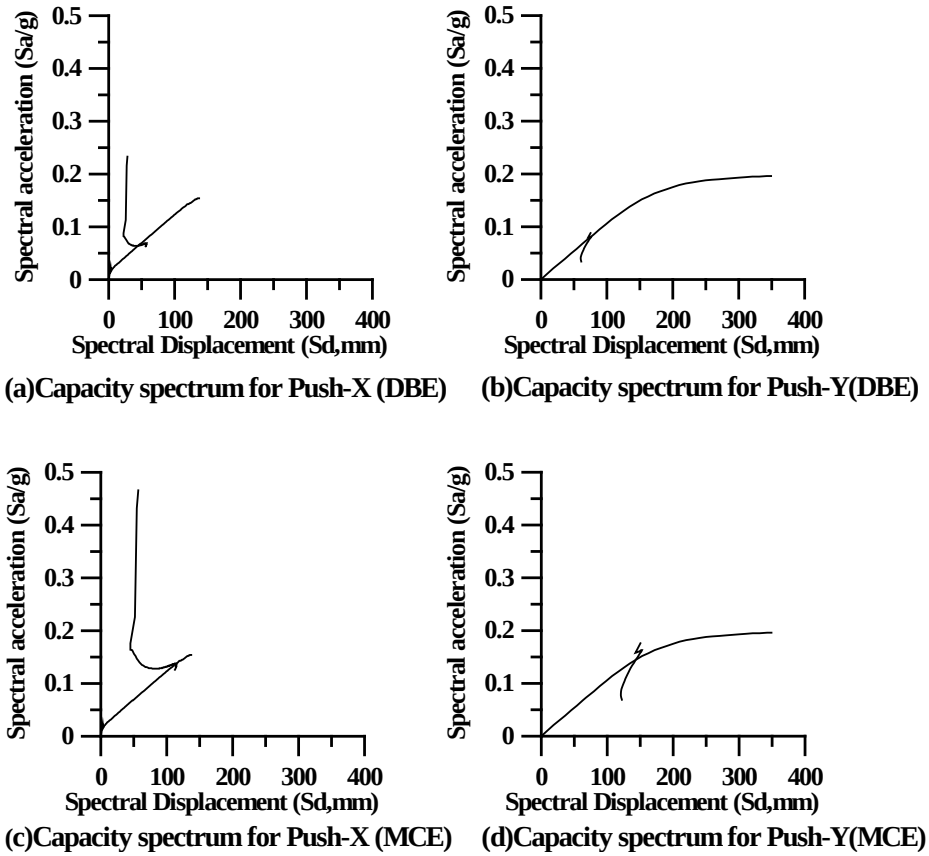

Figure 16. Capacity spectrum for Push-X and Push-Y (DBE, MCE)

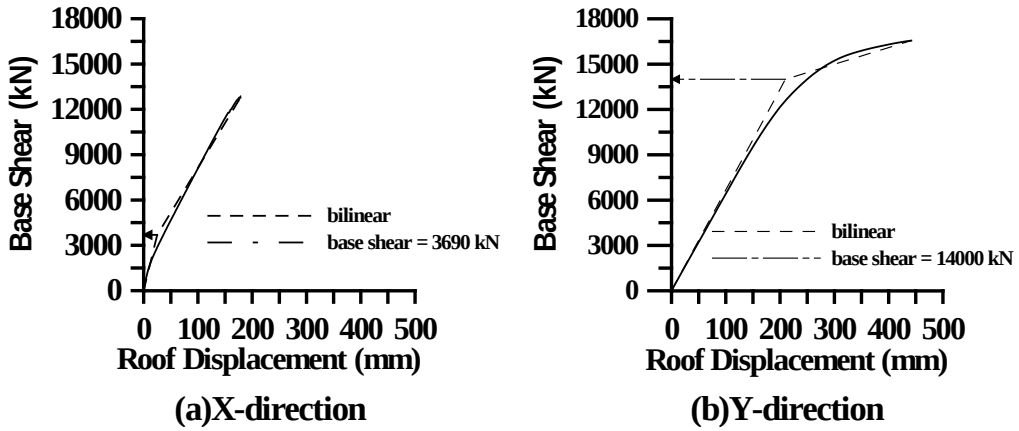

Figure 17. Bilinear representation for the pushover curves

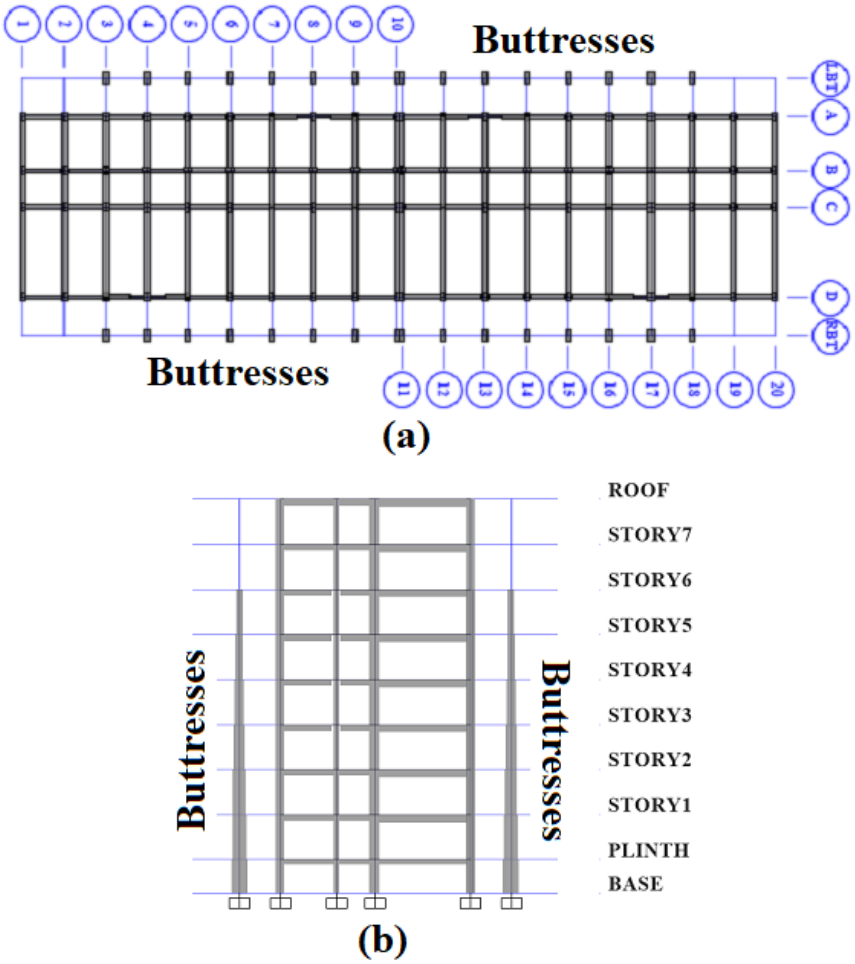

Figure 18. Buttresses locations, (a) Plane, (b) Elevation

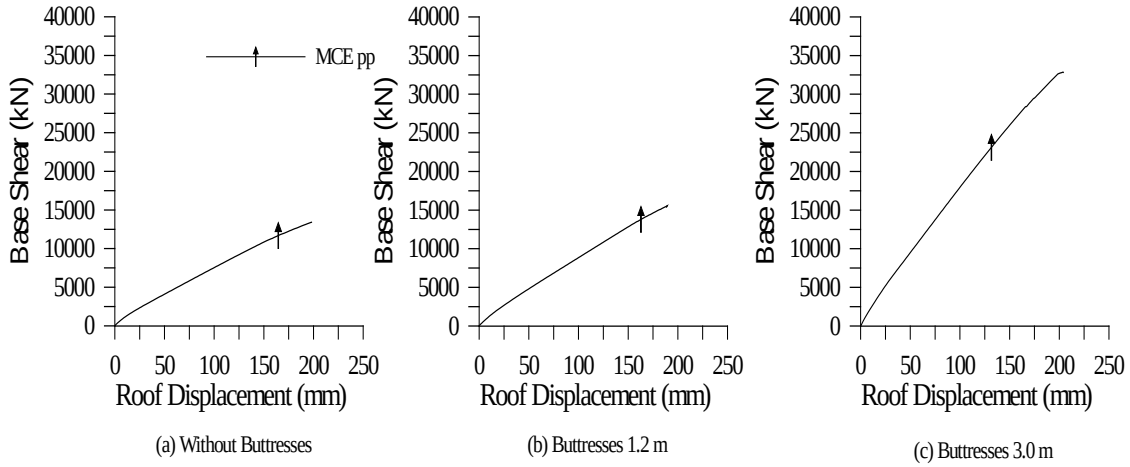

Figure 19. Performance Points for MCE

Table 3. Properties of a typical infill wall

Location of Brick Masonry Infill	The dimension of brick masonry (m)		Cross-section of the equivalent strut (mm)		Frame to wall strength ratio value,β	Yield axial force (kN)	Maximum plastic displacement (mm)
	Length	Height	Width (a)	Thickness (t)			
Above the plinth A-B	3.5	2.95	559	229	>1.3	189	27
Above the plinth C-D	6.4	2.95	953	229	>1.3	290	22
Under the plinth A-B	3.5	2.3	584	229	>1.3	173	20
Under the plinth B-C	2.22	2.3	406	330	>1.3	320	18
Under the plinth C-D	6.4	2.3	965	229	>1.3	290	13
Under the plinth in the longitudinal direction	2.8	2.3	330	330	>1.3	332	18
compressive strength	4.14 MPa	Elastic modulus	2958 MPa	Flexural Tensile Strength	0.069MPa	shear strength	0.138MPa

Table 4. Target displacements at MCE

Frame configuration	Direction	Correction Factors				Effective fundamental period Te (sec)	Target Displacement (mm) by DCM	Target Displacement (mm) by CSM
		C0	C1	C2	C3			
Without buttresses	X	1.5	1.0	1.0	1.0	1.32	164	149
With buttresses 1.2 m	X	1.5	1.0	1.0	1.0	1.244	154	163
With buttresses 3.0 m	X	1.5	1.0	1.0	1.0	1.06	131	122

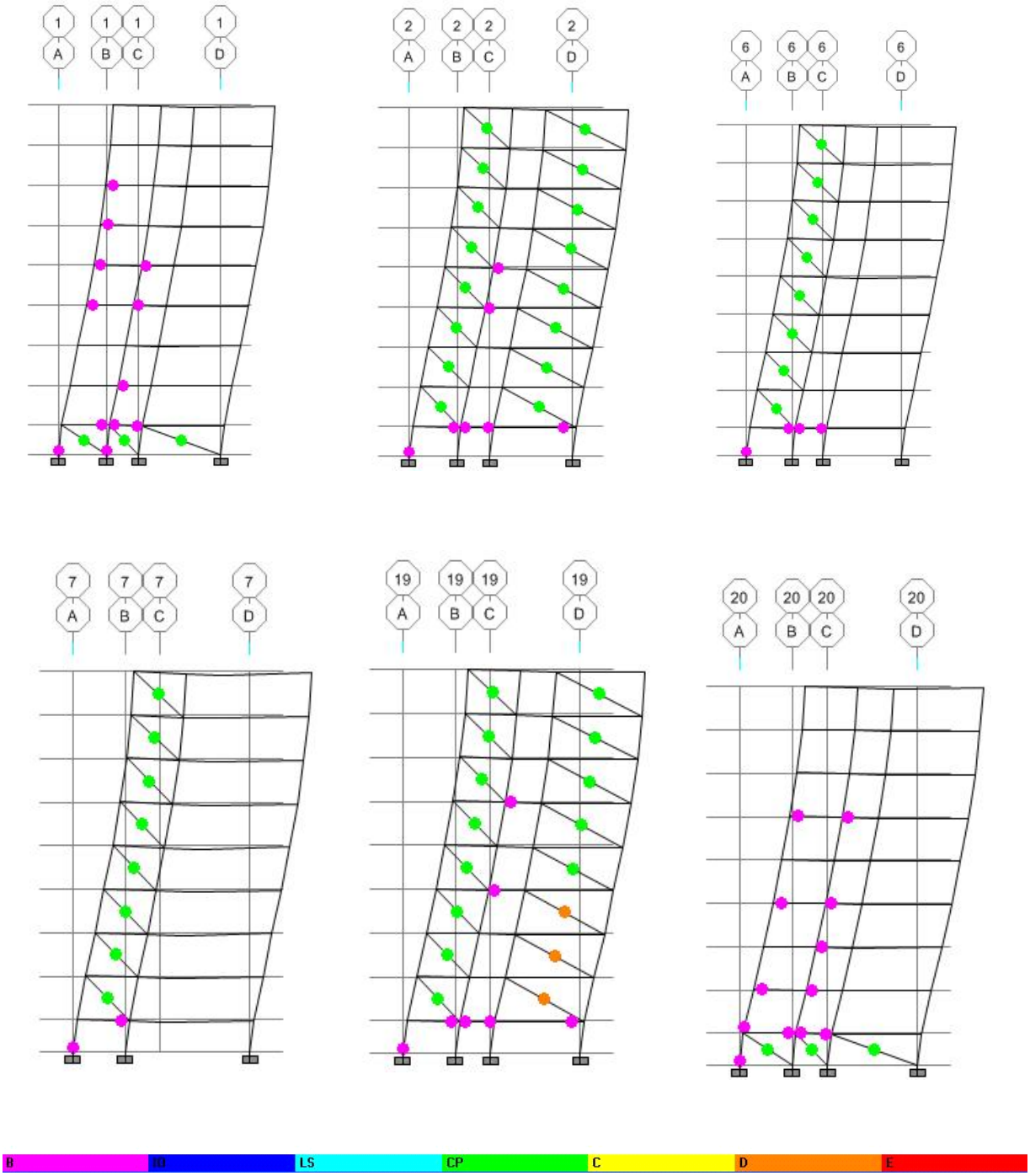

Figure 20. Plastic hinges at performance point under MCE, without buttresses, Pink or blue indicate IO, green indicates CP

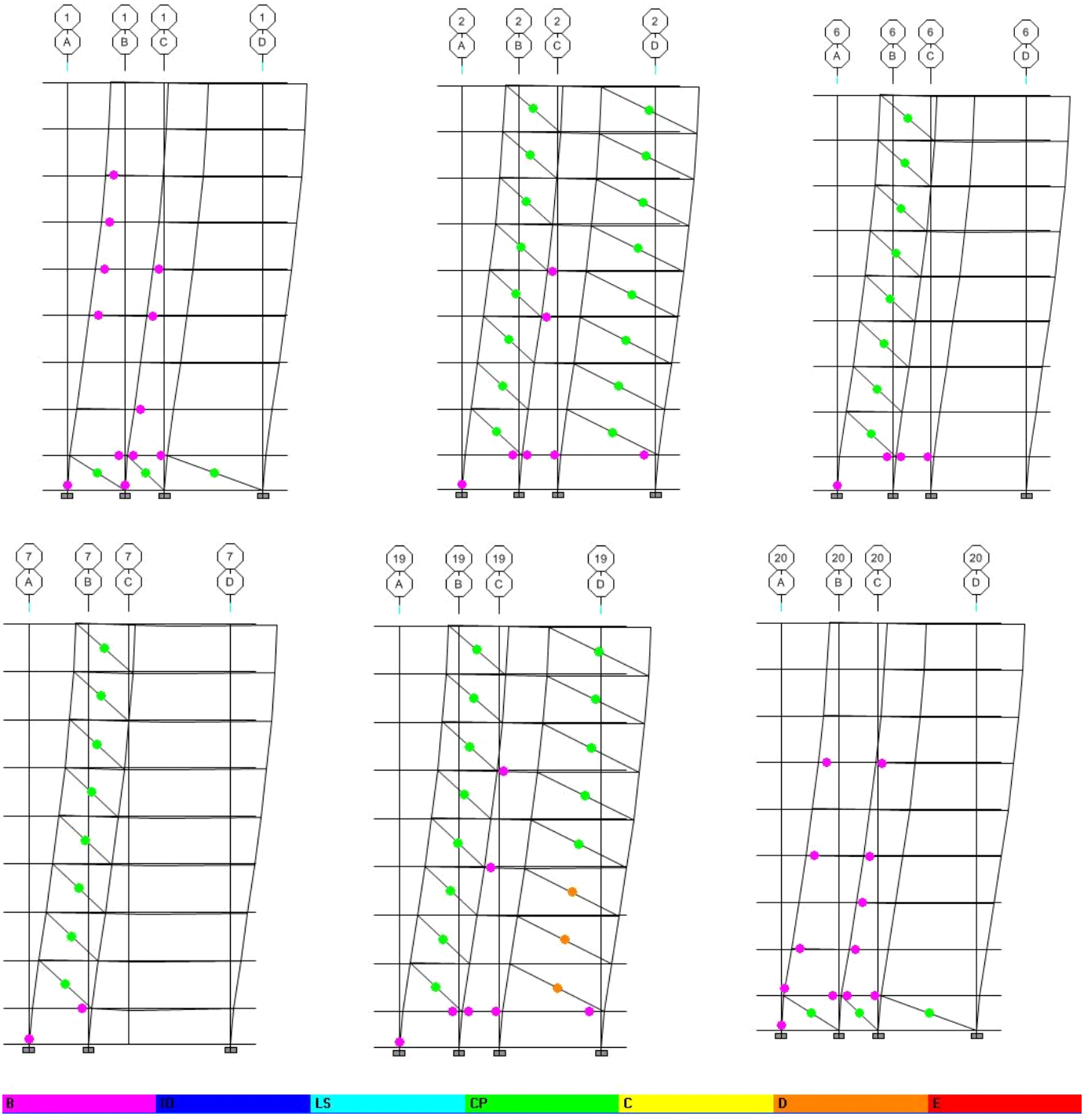

Figure 21. Plastic hinges at performance point under MCE, with 1.2 m buttresses, Pink or blue indicate IO, green indicates CP

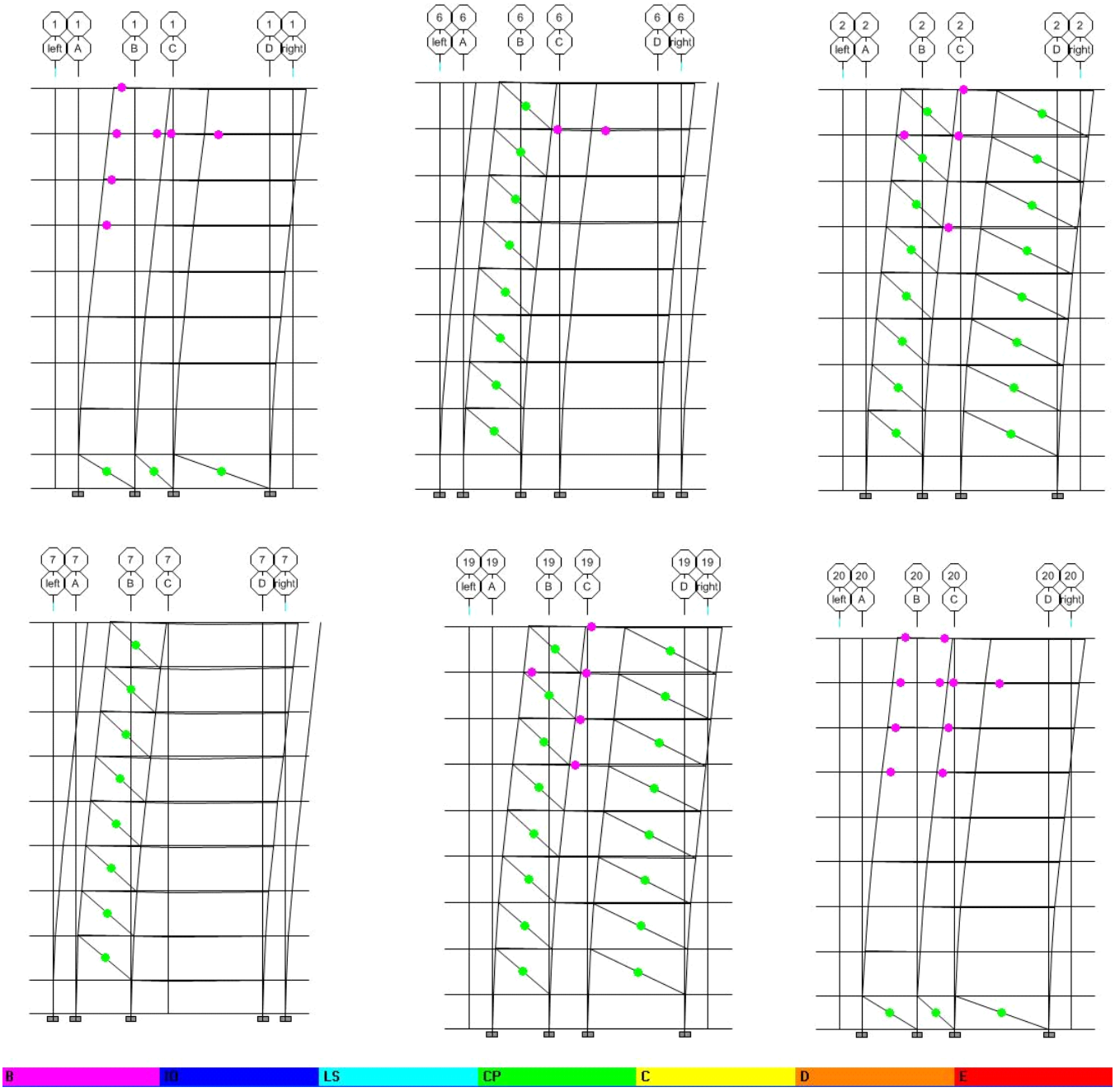

Figure 22. Plastic hinges at performance point under MCE, with 3.0 m buttresses, Pink or blue indicate IO, green indicates CP

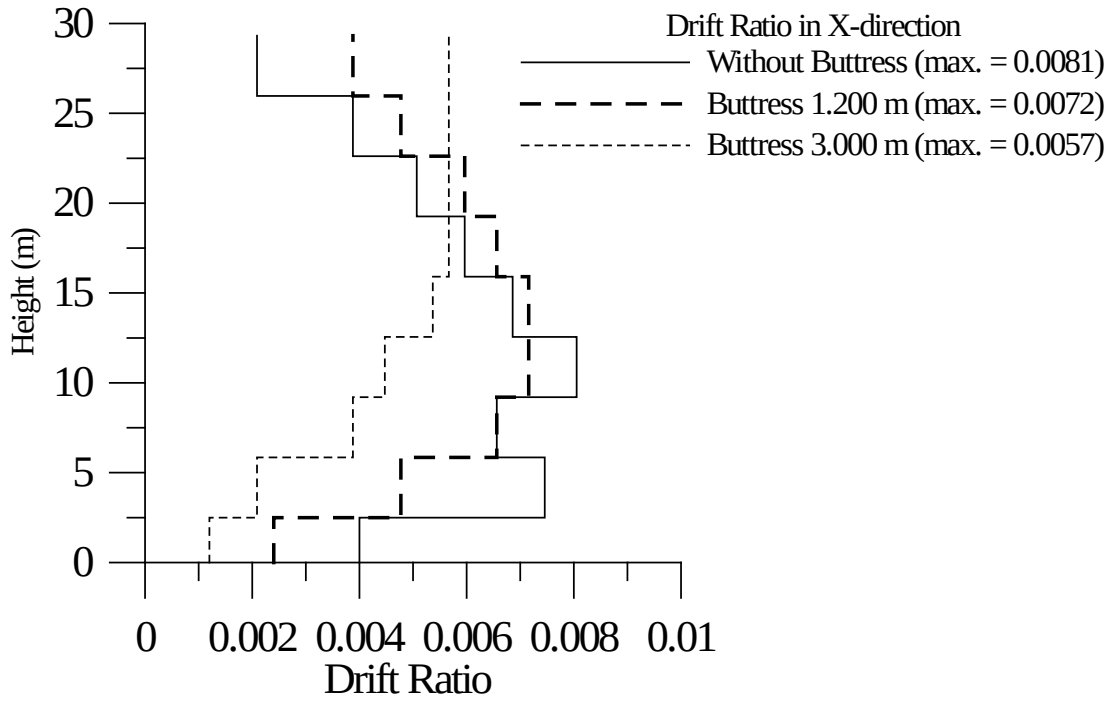

Figure 23. Storey drift ratio for MCE

7. Conclusions and Recommendations

The Capacity Spectrum Method and Displacement Coefficient Method of FEMA 356/ 440 were used to determine the performance level of the Ward block of GTB hospital building by performing nonlinear static pushover analyses. Based on the nonlinear pushover analysis of the Ward block of GTB hospital building, following conclusions can be drawn:

- It was observed that the infills (due to their small number in the considered building) do not make any appreciable effect on the performance level, except their failure at an early stage.
- It was observed that the infills collapse even with 3m wide buttresses.
- The DCM was observed to give slightly higher target displacements, as compared to CSM.
- It was observed in the nonlinear pushover analysis that the unreinforced masonry (URM) infills collapse before the performance point of the building for the Maximum Considered Earthquake (MCE).
- The beams and columns were checked and found safe for the expected shear force at performance point. The columns were also checked and found safe for the shear caused by off-diagonal masonry struts.
- The plastic deformations in individual components were checked for the limits specified by FEMA 356. The beams and columns were found to be within IO performance level while those in masonry infills have crossed CP performance level according to the results of the plastic deformations.

- The inter-storey drift was checked at each storey and the drift ratio was found to be less than 0.01.

The following measures have been recommended to safeguard the wards black buildings against any future earthquake:

1. The building consists of two blocks are separated by a gap of 20 mm. The pounding of the blocks is expected as the gap between the two blocks is insufficient. It was suggested to stitch the two blocks together to avoid any pounding. The analysis was performed for the integrated blocks.
2. As the intervention inside the functioning hospital is extremely difficult, it was explored whether it is possible to safeguard the infills by stiffening the building by providing external buttresses. However, the infills fail even with external buttresses. Therefore, it is not possible to ensure the safety of infills using external interventions and the infills need to be retrofitted locally by providing support against out of plane collapse. One of the suggested measures is strengthening the masonry walls with externally bonded Fiber Reinforced Polymer (FRP) laminates. Other measures may be adding welded wire mesh to avoid the collapse of the masonry in out of the plane and provide positive anchorage into the frame elements by drilling holes, grouting 8ϕ steel rods and weld steel plates/ angles to the grouted rods.

Abbreviations

a	equivalent width of the diagonal member
A_g	gross area
A_w	shear area
C_o, C_1, C_2 and C_3	correction factors
CP	collapse prevention
CSM	capacity spectrum method
DBE	design basis earthquake
DCM	displacement coefficient method
d_{inf}	diagonal length of masonry infill wall
E_c	modulus of elasticity of concrete
E_{fe}	expected modulus of elasticity of frame material
E_{me}	expected modulus of elasticity of
f_a	allowable compressive strength for the masonry wall
f_c	expected compressive strength for the masonry wall
FRP	fiber reinforced polymer
g	ground acceleration
h	height of storey
h_{col}	column height between centerlines of beams
h_{inf}	height of infill panel
I_{col}	moment of inertia of column
I_g	moment of inertia for gross section
IO	immediate occupancy
L_{inf}	length of infill panel
LS	life safety
MCE	maximum considered earthquake
m_i	mass of storey i
n	number of storey
R	reduction factor
R_{dc}	diagonal load at failure for infill wall
r_{inf}	diagonal length of infill panel
S_a	spectral acceleration
t	thickness of masonry wall
T_e	effective fundamental period
URM	unreinforced masonry
V_{bx}	design base shear in x-direction
V_{by}	design base shear in y-direction
δ_t	target displacement
θ	angle whose tangent is the infill height to length aspect ratio, in radians
λ_1	coefficient used to determine equivalent width of infill strut

Conflict of interest

There are not conflicts to declare.

8. References

1. Singh, Y., *"Issues and Challenges In Retrofitting Of Buildings"*, National Programme on Earthquake Engineering Education (NPEEE) Short Term Course on Seismic Evaluation and Retrofit , Coordinators Sing, Y. and Paul, D.K., Department of Earthquake Engineering, Indian Institute of Technology Roorkee, India.
2. ETABS, (1995) Integrated Building Design Software, Computers and Structures, Inc., Berkeley, California, USA.
3. FEMA-356, (2000) *"Prestandard and Commentary for the Seismic Rehabilitation of Buildings"*, Federal Emergency Management Agency, Washington, D.C.
4. FEMA-273, (1997) *"NEHRP Guidelines for the Seismic Rehabilitation of Buildings"*, Federal Emergency Management Agency, Washington, D.C.
5. Applied Technology Council, 1996, *"Seismic Evaluation and Retrofit of Concrete Buildings"*, Report No. SSC 96-01: ATC-40, Vol.1, Redwood City, California.
6. Jarallah, H.K., Singh, Y. and Paul, D. K., (2006) *"Nonlinear Static (Pushover) Analysis of GTB Hospital (Ward Block)"*, Technical Report No. EQ: 2006-10, Department of Earthquake Engineering, Indian Institute of Technology Roorkee, India, 69 p.
7. Bureau of Indian Standards, Bureau of Indian Standards, *"Indian Standard Code of Practice for Plain and Reinforced Concrete"*, (Fourth Revision), IS 456: 2000, New Delhi, India, 100 p.
8. ASCE/SEI 41-06, (2007) *"Seismic Rehabilitation of Existing Buildings"* .
9. FEMA-440, 2004, *"Improvement of Nonlinear Static Seismic Analysis Procedures"*, Federal Emergency Management Agency, Washington, D.C.
10. Bureau of Indian Standards, (2002)*"Indian Standard Criteria for Earthquake Resistant Design of Structures"*, IS 1893: (Part 1) Part 1 General Provisions and Buildings (Fifth Revision), New Delhi, India, 39 p.
11. American Concrete Institute, (2013) *"Building Code Requirements and Specification for Masonry Structures"*, TMS 402-13/ACI 530-13/ASCE 5-13, TMS 602-13/ACI 530.1-13/ASCE 6-13.